42

NBSIR 73-147

Proof Testing of Ceramic Materials--An Analytical Basis for Failure Prediction

A. G. Evans and S. M. Wiederhorn

Inorganic Materials Division
Institute for Materials Research
National Bureau of Standards
Washington, D. C. 20234

March 1973

Interim Report

Prepared for
Office of Naval Research
Department of the Navy
Arlington, Virginia 22217

NBSIR 73-147

PROOF TESTING OF CERAMIC MATERIALS--AN ANALYTICAL BASIS FOR FAILURE PREDICTION

A. G. Evans and S. M. Wiederhorn

Inorganic Materials Division
Institute for Materials Research
National Bureau of Standards
Washington, D. C. 20234

March 1973

Interim Report

This report is to be superseded by a future publication which will receive general distribution and should be cited as a reference. Please consult the NBS Office of Technical Information and Publications to obtain the proper citation.

Prepared for
Office of Naval Research
Department of the Navy
Arlington, Virginia 22217

U. S. DEPARTMENT OF COMMERCE, Frederick B. Dent, Secretary
NATIONAL BUREAU OF STANDARDS, Richard W. Roberts, Director

ABSTRACT

An analysis is presented which permits the accurate prediction of component lifetimes after proof testing. The analysis applies to crack propagation controlled fracture but can be used as a conservative prediction when crack initiation is predominant. The analytical predictions are confirmed in a series of time-to-failure measurements.

1. INTRODUCTION

In many ceramic systems of structural importance,[1-4] slow crack growth precedes fast fracture and this leads to a time dependence of strength. The successful structural exploitation of these materials requires, therefore, a detailed understanding of the time dependent behavior so that accurate failure predictions can be made. The accuracy of failure prediction is very substantially enhanced by incorporating a component proof test prior to service. It is generally considered, therefore, that effective proof testing is an essential prerequisite for the successful structural application of ceramic materials. The primary objective of this paper is to present an analysis based on fundamental principles which enables proof test conditions to be accurately selected, thereby ensuring the "in-service" component lifetimes demanded by a particular application.

The proof test analysis considers a rapid proof test (which does not lead to any significant slow crack growth in the unbroken components) and then a more practically realistic "slow" proof test (which may permit slow growth, and hence, lead to strength degradation in the unbroken components). The predictions of the analysis are then verified in a series of critical experiments. Finally, some general considerations of time dependent fracture in brittle materials are developed, which enable techniques for the rapid evaluation of the important crack propagation parameters to be established.

2. FUNDAMENTAL ASPECTS OF TIME DEPENDENT FAILURE

Fracture involves two independent series processes, flaw initiation and flaw propagation. One of these processes is usually predominant, although it is important to recognize that sometimes both processes contribute in a significant way to failure. In most ceramic materials of structural importance, there are preexisting sharp cracks[5] so that flaw propagation is usually the predominant failure process. A crack propagation analysis will thus predict the time to failure for most ceramic materials (this will be a conservative underestimate when flaw initiation is also necessary).

2.1 Crack Growth Characteristics in Ceramics

It has been established by a number of investigators[1,2,6,7] that for a given system (environment, temperature, material, etc.) there is a unique relation between the crack velocity v and the crack tip stress intensity factor, K_I. For example, in many ceramics the amount of water in the environment has a strong influence on crack propagation.[1,2] Tri-modal K_I-v curves (see figure 1) are then frequently obtained; Regions I and II of the crack propagation curve result from the stress corrosion caused by water in the environment, while Region III is independent of environment.

For most ceramic systems, Region II occurs at a sufficiently high crack velocity that the crack propagation time is controlled almost exclusively by crack growth in Region I. The crack velocity in Region I can generally be expressed as a power function of the stress intensity factor[8]

$$v = AK_I^n. \tag{1}$$

where n and A are constants. n for ceramic materials is always a large number; 9 for Si_3N_4 (1400° C)[9];15-50 for glass[1,10]; 30-40 for porcelain.[9] In contrast to metals, therefore, large changes in velocity result from relatively small changes in K_I. Also, it should be noted that the slow growth limit, K_o, occurs at such low velocities in ceramic materials, $< 10^{-10}$ m/s,[6,10] that its existence has not been generally proven.

2.2 An Estimate of Time-to-Failure from Crack Growth Kinetics

The crack growth kinetics (fig 1) can be used for predictions of time-to-failure under constant load. The time, t, required for a crack to propagate from subcritical to critical size is easily derived from the definition of crack velocity, da/dt = v (where a is the crack length), and the usual relationship between stress intensity, applied load, σ_a, and crack length; $K_I = \sigma_a Y\sqrt{a}$ (where Y is a geometric factor).[11] This gives;[6]

$$t = (2/\sigma_a^2 Y^2) \int_{K_{Ii}}^{K_{If}} (K_I/v)\,dK_I \tag{2}$$

where K_{Ii} and K_{If} are the initial and final values of the stress intensity factor. Using the relationship for crack velocity from eqn (1);

$$t = 2(K_{Ii}^{2-n} - K_{If}^{2-n})/\left[(n-2)A\sigma_a^2 Y^2\right] \tag{3}$$

Furthermore, since failure is essentially instantaneous when $K_{If} = K_{IC}$, then the time to failure, τ, is given by,

$$\tau = 2(K_{Ii}^{2-n} - K_{IC}^{2-n})/\left[(n - 2)A\sigma_a^2 Y^2\right] \quad (4)$$

Also, since $9 < n < 50$ for ceramic materials, $K_{IC}^{2-n} << K_{Ii}^{2-n}$ for the usual range of load application ($K_{Ii} < 0.9\ K_{IC}$), and the following equation holds as a good practical approximation:

$$\tau \simeq 2K_{Ii}^{2-n}/\left[(n - 2)\ A\sigma_a^2 Y^2\right] \quad (5)$$

Thus, the time-to failure is determined provided K_{Ii}, the initial stress intensity factor at the largest flaw, and the $K_I - v$ curve are known.

3. FAILURE PREVENTION BY PROOF TESTING

3.1 Analytical Predictions

3.1.1 Time-to-Failure After Proof Testing

As demonstrated by Tiffany and Masters,[12] Wiederhorn,[13] and Tetelman,[14] an upper limit to K_{Ii} and, consequently, a lower limit to the time-to-failure can be obtained by proof testing. Survival of the proof test guarantees that the stress intensity factor at the tip of the most serious flaw does not exceed K_{IC}, otherwise failure would have occurred. Thus, $K_{Ii}/\sigma_a = (K_I)_{proof}/\sigma_p < K_{IC}/\sigma_p$. Substituting $K_{Ii} < \sigma_a K_{IC}/\sigma_p$ into eqn (5) as the maximum value for the initial stress intensity factor, the following equation is obtained for the minimum time to failure

$$\tau_{min} = 2(\sigma_p/\sigma_a)^{n-2}/\left[(n - 2)A\sigma_a^2 Y^2 K_{IC}^{n-2}\right] \quad (6)$$

It is apparent that τ_{min} depends on the proof stress/ to applied stress ratio and independently upon the magnitude of the applied stress(for a given system). It is thus possible to represent the minimum failure time for any system in graphical form as a series of parallel lines on logarithm time, stress coordinates, with the position of the line depending only on the ratio σ_p/σ_a (for a given system). An example for soda-lime glass in water (using K_I - v data from ref 10) is shown in fig 2. It is immediately apparent from the diagram what level of proof stressing is needed to guarantee no failures within a specified time at the operating load.

More importantly, diagrams of this type can be used to select materials for a specific application. For example, if a lifetime of 10^5 seconds at an operating stress of 100 MNm^{-2} (14,000 psi) are the requirements, this can only be assured using soda-lime glass (fig 2) if the components are proof tested at 400 MNm^{-2} ($\sigma_p/\sigma_a = 4$); the soda-lime glass component should therefore have a fast fracture stress of 400 MNm^{-2} at an acceptable failure probability (e.g. < 1%) so that excessive breakages during the proof test are avoided. If this is not possible, then that application should be regarded as inadmissible for soda-lime glass, and another material should be considered.

The minimum time to failure predicted in this way may, in fact, be substantially lower than the observed failure time for most components, due to the wide distribution of strengths, and hence failure times. When a certain level of failure during service is acceptable, therefore, it is often possible to allow the components to remain in service for periods much longer than τ_{min}. A formal treatment of this can be developed as follows, by combining fast fracture strengths with the time-to-failure parameters (c.f. section 4.1).

The time to failure in excess of the minimum may be obtained directly from eqn (5), and is given by,

$$\frac{\tau}{\tau_{min.}} = \left(\frac{\sigma_f}{\sigma_p}\right)^{n-2} = R^{n-2} \qquad (7)$$

where σ_f refers to the component fracture stress after proof testing. Values of τ usefully larger than τ_{min} are thus obtained for $\sigma_f \gtrsim 1.5\,\sigma_p$. The strengths after proof testing may be found quite simply from the original strength distribution. Consider the typical distribution shown in fig 3†. Proof testing to a stress, σ_p, eliminates all components with lower strengths. This attenuates the distribution of the remaining strengths, as shown by the dotted line in fig 3. The failure probability P_a for the attenuated distribution is derived from,[15]

$$P_a = \frac{P_i - P_P}{1 - P_P} \qquad (8)$$

where P_i is the initial failure probability and P_P is the failure probability at the proof stress. It is apparent from fig 3 that the magnitude of τ/τ_{min} depends essentially on the ratio of the number of components that can be permitted to break in service, P, to the number that break during the proof test, P_P. If only a small number of component failures can be permitted, such that $P < P_P$, then $\sigma_f \approx \sigma_p$ (fig 4), $R \approx 1$ (see R_1), and τ_{min} is the only acceptable failure time. If a larger number of component failures are allowed, $P \approx P_P$, $R >> 1$ (see R_2) and τ can be larger than τ_{min} by several orders

---

†Weibull axes[15] are used for convenience of presentation; this does not mean, of course, that the analysis is confined to strengths that fit this type of distribution.

of magnitude. Finally, for $P > P_p$, (see R_3) the significance of τ_{min} is lost because τ is many orders of magnitude larger and proof testing is no longer a useful prerequisite to component application. These conclusions are expressed in analytical form for a Weibull strength distribution in Appendix II.

3.1.2 Strength After Proof Testing

Thus far, it has been considered that proof testing is not accompanied by slow crack growth. This can only be achieved if the proof test is conducted vary rapidly, or in the absence of the slow growth medium. Normally, however, some slow crack growth is expected to occur during the proof test. An analysis of the extent of this slow crack growth and its effect on strength and time to failure is clearly needed to develop a complete appreciation of the consequences of proof testing.

The degree of weakening due to crack growth is easily obtained from equation (3). Defining K_A as

$$K_A^{2-n} \equiv (n - 2)A\sigma_a^2 Y^2 t/2 \qquad (9)$$

eqn (3) becomes

$$K_A^{2-n} = K_{Ii}^{2-n} - K_{If}^{2-n} \qquad (10)$$

For $K_{If} = K_{IC}$, the condition for failure becomes

$$(K_{Ii}^*)^{2-n} = K_A^{2-n} + K_{IC}^{2-n} \qquad (11)$$

where K^*_{Ii} is the critical (i.e. the smallest) value of initial stress intensity factor that results in failure during the proof test. Substituting eqn (11) into (10), the relative change in crack tip stress intensity factor during loading is given by

$$(K_{Ii}/K_{If})^{n-2} = 1 - (K_{Ii}/K^*_{Ii})^{n-2}[1 - (K^*_{Ii}/K_{IC})^{n-2}] \tag{12}$$

The relative change in specimen strength due to proof testing can be determined from eqn (12).† Since the stress during proof testing, σ_P, is constant, $K_{Ii}/K_{If} = \sqrt{a_i/a_f}$, where a_i and a_f are the flaw sizes before and after proof testing. Also, since fast fracture occurs when $K_I = K_{IC}$, the fast fracture strengths after proof testing are given by, $\sigma_f/\sigma^*_f = \sqrt{a_f/a_i}$, where σ_f is the strength if no slow crack growth had occurred during proof and σ^*_f is the actual strength after proof. Similarly, it may be shown that $K_{Ii}/K^*_{IC} = \sigma^*_P/\sigma_f$, where σ^*_p is the equivalent fast fracture proof stress, and $K^*_{Ii}/K_{IC} = \sigma_P/\sigma^*_P$. These various stress parameters are shown in fig 4 using strength data for E-glass fibers.[17] Substituting stresses for stress intensity factors in eqn (12), the following equation is obtained for the relative strength degradation

$$\left(\frac{\sigma_f^*}{\sigma_f}\right)^{n-2} = 1 - \left(\frac{\sigma_p^*}{\sigma_f}\right)^{n-2}\left[1 - \left(\frac{\sigma_p}{\sigma_p^*}\right)^{n-2}\right] \tag{13}$$

†The strengths referred to here are fast fracture strengths, whereas the strengths measured in practice will often be lower than the fast fracture strength due to slow crack growth during the test. This difference is dependent on the strain rate used for strength measurements, and the effect can be predicted with good accuracy from the K_I - V diagram for the system, (see section 4.2).

The strength distribution of the components that remain after proof testing can thus be obtained quite simply from the original distribution of fast fracture strengths. Values of σ_f^* calculated for the E-glass fibers (obtained for n = 12) are shown in fig 4. The predicted curve is in very good agreement with actual strength measurements made after proof testing.†

In addition, it should be noted that the strength after proof testing is larger at all levels of failure probability than the original strength prior to the proof test. This result can be expressed in analytical form for a Weibull distribution (Appendix I) by; $\sigma_f^* > \sigma_i$ (the original strength) when $m < (n-2)$, where m is a constant related to the strength distribution[16] (small m corresponding to a wide distribution). This condition will be satisfied for most ceramic systems of structural importance.

The slow crack growth during the proof test also has an effect on the time to failure. The minimum failure time is not affected because the condition that $K_{If} < K_{IC}$ after proof testing still applies. The strength σ_f^* must be used however to evaluate $\tau > \tau_{min}$, by substituting σ_f^* for σ_f in eqn (7).

---

†The data shown in fig 4 have been used to show that no slow growth occurs during the proof test.[17] This conclusion can only be correct if the flaws that control fast fracture do not contribute in any way to the time dependent fracture--a most unlikely situation.

3.2 Experimental Verification

Experiments are designed to verify the lifetime predictions provided by the preceding analysis. In these, ground specimens of soda-lime glass are proof tested in water and the times to failure after proof testing are measured. Both fast fracture and constant load proof testing are used.

3.2.1 Fast Fracture Proof Test

For the fast fracture proof test, the return and gauge length controls of an Instron testing machine are preset so that the load will increase rapidly to a predetermined value and then reduce immediately to a fixed proportion of the maximum. The subsequent time to failure is then measured on the chart. A proof stress/applied stress ratio of 1·35 is selected for convenience. The results are plotted on a proof test diagram (fig 5) where they are compared with the predicted minimum failure time. All of the measured times lie above the predicted τ_{min} line, which verifies the position of the line as, at least, a conservative estimate of observed τ_{min}. A more precise test of the analytical predictions is provided by estimating failure times on a probability basis and comparing these with measured times. Values for τ/τ_{min} are obtained from the distribution of fast fracture strengths (fig 6) in conjunction with the analysis in Appendix II. A total of 50 specimens were tested at each of two stress levels, 45 and 9 MNm^{-2}, so that the weakest specimen in each series has a failure probability of ~0.02. The magnitude of τ is thus evaluated for P = 0.02, and plotted in fig 5. The measured time to failure of the weakest specimen at each stress is in close agreement with the predicted time to failure, showing that the analytical predictions are of good accuracy and not excessively conservative.

3.2.2 Constant Load Proof Test

In the constant load proof test, the proof stress was applied for 5 minutes and then the load reduced to the applied stress level, again using $\sigma_p/\sigma_a = 1{\cdot}35$. The measured failure times are shown in fig 5 for $\sigma_a \approx 15$ MNm^{-2}. The data lie above the predicted τ_{min}. Using appropriate values of σ_p^* and n, σ_f^* (and hence τ) may be calculated. The value of τ obtained (fig 5) for P = 0.02 is again entirely consistent with the measure of failure times at equivalent probability.

4. CRACK PROPAGATION PARAMETERS

The value of proof testing as a means of assuring reliability depends on the accuracy of both the crack propagation parameters and the statistical parameters needed to describe strength. Statistical parameters are used to predict probability of failure under static loading (see section 3.1.1), and for lifetime predictions of parts that have been subject to momentary overloads during use.† Statistical parameters can be obtained experimentally

---

† Here, the overload is treated as the proof test load and the treatment of section 3.1.1 is followed.

from strength data that has been treated, for example, by the normal or Weibull type distributions. In practice, it is important that these experimentally determined parameters reflect the materials being used if proof test predictions are to be reliable.

Crack propagation parameters can be determined in a number of ways. The most direct method is to measure the crack velocity as a function of stress intensity factor. When using crack velocity methods to determine crack propagation parameters, one must be sure that environmental conditions at the tips of large cracks are identical to those at tips of the small cracks normally present in ceramic materials. The crack propagation parameters can also be determined using strength measurement techniques. These have the advantage that the parameters are determined for the same flaws that control strength; their disadvantage is that crack propagation parameters have to be inferred from the data without actually viewing the crack motion; in addition, detailed information on K-v curves cannot be easily obtained. Nevertheless, when agreement is obtained between the crack propagation and strength techniques of measuring crack growth parameters, one is assured of an accurate prediction of lifetimes under load.

Both time-to-failure measurements at constant load,[10,18] and the strain rate dependence of strength[8,18] can be used to obtain the crack propagation parameters. Conventionally, these have entailed a laborious series of measurements to obtain average values of time to failure or strength, making some assumption concerning the strength distribution. Modified methods for handling the data enable much more efficient procedures to be developed, which take proper account of the statistical variations in strength. These methods require a consideration of probability relationships between fast and slow fracture and the application of these to crack growth data, as described below.

4.1 Probability Aspects of Time Dependent Failure

When crack propagation controls fracture, the flaws controlling strength are usually identical for both fast fracture and time dependent fracture. It is quite acceptable, therefore, to combine an analysis of failure probabilities, P, measured for fast fracture with independent measurements of slow crack growth in order to describe the statistical nature of failure times. This may be expressed in mathematical form as:

$$P = \Lambda(\sigma_{IC}) \tag{14}$$

where $\Lambda(\sigma_{IC})$ is a function of the fast fracture strength, σ_{IC}. The time to failure is related to the fast fracture strength and the applied stress, σ_a, by

$$\frac{\sigma_a}{\sigma_{IC}} = T(t) \tag{15}$$

where T(t) is a dimensionless function of time. Combining eqns (14) and (15) at constant σ_{IC} gives the probability of failure in time t;

$$P = \Lambda\left(\frac{\sigma_a}{T(t)}\right) \tag{16}$$

4.2 Constant Strain Rate Technique

The principles developed in section 4.1 will now be applied to the constant strain rate technique of determining crack propagation parameters. The fracture stress σ at constant strain rate $\dot{\varepsilon}$ is given for relatively small cracks by[8]

$$\sigma = \frac{K_o}{Y\sqrt{C_o}}\left[1 + \frac{2YE\dot{\varepsilon}(n+1)C_o^{3/2}}{V_oK_o(n-2)}\right]^{1/(n+1)} \tag{17}$$

This reduces to

$$\sigma = B\dot{\varepsilon}^{1/(n+1)}\sigma_{IC}^{(n-2)/(n+1)} \tag{18}$$

where B is a constant. The ratio of the strengths of specimens tested at a strain rate $\dot{\varepsilon}_1$ to the strengths at a strain rate $\dot{\varepsilon}_2$ is thus,

$$\frac{\sigma_1}{\sigma_2} = \left(\frac{\dot{\varepsilon}_1}{\dot{\varepsilon}_2}\right)^{1/(n+1)}\left(\frac{\sigma_{IC_1}}{\sigma_{IC_2}}\right)^{(n-2)/(n+1)} \tag{19}$$

At equivalent failure probabilities, $\sigma_{IC_1} \approx \sigma_{IC_2}$ † so that eqn (19) reduces to:

$$\log \sigma_2 = \log \sigma_1 - \frac{1}{(n+1)} \log\left(\frac{\dot{\varepsilon}_1}{\dot{\varepsilon}_2}\right) \qquad (20)$$

This relationship suggests a very simple experiment in which N strength measurements are made at each of two separate strain rates, and the strengths ranked in increasing order (the lowest strength first, the next lowest second, etc.) The strengths for constant rank are then plotted on logarithmic axes. This should yield a linear plot with a slope of unity and an intercept that gives n. Results obtained for ground soda-lime glass tested in water are plotted in fig 7. An attractive feature of this technique (apart from its simplicity and rapidity) is that it permits an immediate comparison of the strength distributions in the two series of specimens. If the data generate a plot with a slope that differs significantly from unity, this shows that the two distributions are not comparable (due to differences in flaw size distributions), thereby invalidating the experiment, and suggesting a closer control of specimen preparation. This, therefore, eliminates misleading results due to variables in specimen preparation and, equally important, enables good data to be obtained with the minimum of testing. The experiments on glass, for example, indicated that 20 specimens at each strain rate are adequate.

---

†The equivalence is not exact because a certain confidence level must be applied to each probability, and this depends on the total number of tests performed.

A value for B is found from an additional N fast fracture strength measurements to obtain σ_{IC}. These measurements must be performed either at high strain rate, or in the absence of the corrosive environment, to eliminate all slow crack growth prior to fast fracture. Then a plot of log σ vs log σ_{IC} at equivalent probability enables B to be evaluated from:

$$\log \sigma = \left(\frac{n-2}{n+1}\right) \log \sigma_{IC} + \frac{1}{(n+1)} \log \dot{\varepsilon} + \log B \tag{21}$$

Again, measurements of the slope, (n-2)/(n+1), can be used to check the validity of the experiment.

Values for n obtained for ground soda-lime glass in water, using this technique (fig 7), can be compared with crack velocity data obtained for an identical glass composition and environment.[10,6] There is good correspondence (n = 15 in both cases) indicating that time dependent fracture is predominately propagation controlled in this system.

4.3 Constant Stress Techniques

When constant strain-rate equipment is not available, the relevant information can be obtained using constant stress experiments, although this does involve much longer test times for data acquisition.

A complete set of time-to-failure parameters can be obtained by evaluating times to failure for two series of N specimens at two separate stress levels, σ_{a1} and σ_{a2}, in conjunction with fast fracture strength measurements on a further series of N specimens. Equating failure probabilities at the two stress levels gives (from eqn (5)):

$$\log \sigma_{a_2} = \log \sigma_{a_1} + \frac{1}{n} \log\left(\frac{t_1}{t_2}\right) \tag{22}$$

A plot of the logarithm of the stresses should thus generate a curve with a slope of unity and an intercept which gives a value for n. Then a plot of failure times against fast fracture strengths, at constant probability, gives a value for the constant A in eqn (1).

5. SUMMARY

An analysis is presented which enables accurate predictions to be made of component lifetimes after proof testing, when fracture is crack propagation controlled. It is envisaged that the analysis will be used to design proof tests that will guarantee a minimum lifetime for a component in service.

In most ceramic materials of structural importance, it appears that fracture is predominantly propagation controlled, so that the analysis can be used directly. If examples of fracture controlled by sharp crack initiation occur, then the analysis can be used to give a conservative estimate of lifetime.

Application of the analysis requires values of the crack propagation parameters, n and A (eqn 1) for the prospective material. These can be obtained directly from crack velocity measurements. It is suggested, however, that the parameters be confirmed from strength measurements (at two separate strain rates) to ensure that the crack tip environment is equivalent for the small preexisting cracks and the large through cracks used for velocity measurements.

Experimental confirmation of the accuracy of the analytical lifetime predictions after proof testing is obtained from a series of time-to-failure experiments.

APPENDIX I

THE STRENGTH AFTER PROOF TESTING

It is intuitively expected that the relationship between the strength after proof testing and the initial strength will depend on the amount of slow crack growth during the proof test and the width of the strength distribution. A formal analysis of this effect is described here.

Consider that the strength data can be fitted to a Weibull distribution[15] so that the parameter m can be used as a measure of the strength variation. The initial distribution is given approximately by:[19]

$$\ell n \ell n \left(\frac{1}{1-P}\right) = m \ell n \sigma_i + J \tag{A1}$$

where σ_i are the initial strengths and J is a constant. The strengths after proof test, σ_f^*, will be larger than the strength prior to proof, σ_i, when the following condition is satisfied (see fig 4):

$$\frac{\ell n[-\ell n(1-P_i)] - \ell n[-\ell n(1-P_a)]}{\ell n\sigma_f - \ell n\sigma_f^*} > m \tag{A2}$$

Substituting for P_a from eqn (8):

$$\frac{\ell n[1 - \ell n(1-P_p)/\ell n(1-P_i)]}{\ell n(\sigma_f^*/\sigma_f)} > m \tag{A3}$$

Substituting for σ_f^* from eqn (13),

$$\frac{\ell n[1 - \ell n\,(1 - P_p)/\ell n(1 - P_i)]}{\frac{1}{(n-2)}\,\ell n\,[1 - (\sigma_p^*/\sigma_f)^{n-2}]} > m \qquad \text{(A4)}$$

From eqn (A1),

$$-\ell n(1 - P) = \sigma^m e^J \qquad \text{(A5)}$$

Therefore,

$$\frac{\ell n\,(1 - P_p)}{\ell n\,(1 - P_i)} = \left(\frac{\sigma_p^*}{\sigma_f}\right)^m \qquad \text{(A6)}$$

Substituting for P in eqn (A4) gives,

$$\frac{\ell n\,[1 - (\sigma_p^*/\sigma_f)^m]}{\ell n(1 - (\sigma_p^*/\sigma_f)^{n-2}]} > \frac{m}{n-2} \qquad \text{(A7)}$$

Since $\sigma_p^* < \sigma_f$, this condition is always satisfied provided

$$m < (n-2) \qquad \text{(A8)}$$

The validity of this condition can be easily verified, using the data in fig 4 (where $m = 10$) by calculating σ_f^* for various n. This shows that $\sigma_f^* > \sigma_i$ for $n > 11$ and $\sigma_f^* < \sigma_i$ for $n < 11$, which is entirely consistent with the predictions of eqn (A8).

APPENDIX II

TIME-TO-FAILURE PROBABILITIES

1. TIMES TO FAILURE WITHOUT PROOF TESTING

If the time to failure (eqn 5) is combined with the fast fracture probability (eqn A1), it is possible to obtain the time to failure, τ_o, on a probability basis. From (eqn 5),

$$\tau_o = \frac{2\,\sigma_i^{n-2}}{A\sigma_a^{n} Y^2 (n-2) K_{IC}^{n-2}} \qquad \text{(A9)}$$

Substituting for σ_i from eqn (A1), and taking logarithms,

$$\log \tau_o = \frac{(n-2)}{m} \log \log \left(\frac{1}{1-P_i}\right) - n \log \sigma_a - \frac{J}{m} + \log \left[\frac{2}{A(n-2)Y^2 K_{IC}^{n-2}}\right] \qquad \text{(A10)}$$

For $P_i < 0.1$, this reduces to,

$$\log \tau_o = \frac{(n-2)}{m} \log P_i - n \log \sigma_a - \frac{J}{m} + \log \left[\frac{2}{A(n-2)Y^2 K_{IC}^{n-2}}\right] \qquad \text{(A11)}$$

The values of time to failure without proof testing can thus be plotted on the proof stress diagrams (fig 2) for various P_i as a series of parallel lines (with slope, -n), as shown in fig 8 for ground soda-lime glass. It is immediately apparent from this type of diagram the range of stress levels in which proof testing is a useful prerequisite to component application. It is important to note, however, that the strength parameters must be those applicable to the component, i.e. a volume correction should be applied if strengths are measured on smaller specimens.

2. TIMES TO FAILURE AFTER PROOF TESTING

An analytical expression for the time to failure after proof testing in excess of the minimum, τ/τ_{min}, can be obtained by combining eqn (7) with the fast fracture probability eqn (A1). Since the probability of fracture after proof testing, P_a, tends to zero as the strength, σ_f, tends to the proof stress, σ_p, substitution for P_i from eqn (8) into eqn (A1) gives,

$$\log\left[\frac{-\log(1-P_a)-\log(1-P_p)}{-\log(1-P_p)}\right] = m\log\left(\frac{\sigma_f}{\sigma_p}\right) \qquad \text{(A12)}$$

Substituting for σ_f/σ_p from eqn (7), this reduces for small P_a, P_P (< 0.1) to

$$\log\frac{\tau}{\tau_{min}} = \frac{(n-2)}{m}\log\left[1+\frac{P_a}{P_P}\right] \qquad \text{(A13)}$$

The time to failure is only significantly in excess of the minimum, therefore, for $P_a > P_P$, and provided $(n-2)/m$ is a relatively large number. For ground soda-lime glass $(n-2)/m \simeq 5$, so that the effect is substantial, as shown in fig 8 for the specific example $P_a = 10^{-1}$, $\sigma_p/\sigma_a = 2$. When $P_a \gg P_P$, eqn (A13) reduces to eqn (A11) so that $\tau \rightarrow \tau_o$; when $P_P \gg P_P$, eqn (A13) shows that $\tau \rightarrow \tau_{min}$, as depicted in fig 8.

REFERENCES

1. S. M. Wiederhorn, J. Am. Ceram. Soc. 50, 407 (1967).
2. S. M. Wiederhorn, Intl. Jnl. Frac. Mech. 4, 171 (1968).
3. F. F. Lange, to be published.
4. P. Marshall, Special Ceramics 4, 191 (1968).
5. See for example, A. G. Evans and G. Tappin, Proc. Brit. Ceram. Soc. 20, 275 (1972).
6. A. G. Evans, Intl. Jnl. Frac. Mech. - to be published.
7. K. Schönert, H. Umhauer and W. Klemm, "Fracture - 1969" (Ed. P. L. Pratt), Chapman & Hall, London (1969).
8. A. G. Evans, submitted to Intl. Jnl. Frac. Mech.
9. A. G. Evans and M. Linzer, to be published.
10. S. M. Wiederhorn and L. H. Bolz, J. Am. Ceram. Soc. 53, 543 (1970).
11. W. F. Brown and J. E. Srawley, ASTM, STP410 (1967).
12. C. F. Tiffany and J. N. Masters, ASTM, STP-381 (1964) p. 249.
13. S. M. Wiederhorn, J. Am. Ceram. Soc., to be published.
14. A. S. Tetelman, U.C.L.A. - Eng. 7249, July 1972 (Presented at U.S.-Japan Joint Symposium on Acoustic Emission, Tokyo, Japan).
15. W. Weibull, Ing. Veternskaps Akad. APYEA, Handlinger 15, 153 (1939).
16. W. Weibull, J. Appl. Mech. 18, 293 (1951).
17. G. K. Schmitz and A. G. Metcalfe, I&EC Product Research and Development 5, 1 (1966).
18. J. E. Ritter and C. L. Sherburne, J. Am. Ceram. Soc. 54, 601, (1971).
19. See for example N. A. Weil and I. M. Daniel, Jnl. Am. Ceram. Soc. 47, 269 (1964).

FIGURE CAPTIONS

Fig. 1. Schematic representation of the effect of crack tip stress intensity, K_I, on crack velocity, V, during slow crack growth.

Fig. 2. A proof test diagram for soda-lime glass in water. The numbers below each line refer to the proof stress/applied stress ratio (σ_p/σ_a) corresponding to that line.

Fig. 3. A typical strength distribution for a ceramic material plotted on Weibull axes. σ_p is the proof stress, σ_a is the applied stress and P_1, P_2, and P_3 are different levels of component failure probability. The quantities R_1, R_2, and R_3 are related to the time to failure ratio, τ/τ_{min}.

Fig. 4. The strength of E glass fibers before and after a constant stress proof test at σ_p. Also shown are the strengths after proof testing when no slow crack growth occurs, σ_f, and the predicted strengths due to slow crack growth, σ_f^*. Data obtained from ref (17).

Fig. 5. A comparison of failure times after proof testing for ground soda-lime glass in water, with the predicted minimum failure time for the soda-lime glass/water system (full line), and the times in excess of the minimum for a probability of 0.02.

Fig. 6. The flexural strength distribution of ground soda-lime glass.

Fig. 7. A logarithmic plot of the strengths, σ, and σ_2 at equivalent probability at two separate strain rates, $\dot{\varepsilon}_1$ and $\dot{\varepsilon}_2$ (where $\dot{\varepsilon}_1/\dot{\varepsilon}_2 = 600$). The intercept gives a value for n of 15 ±2.

Fig. 8. A complete time to failure diagram for ground soda-lime glass immersed in water, under a flexural load. The minimum time to failure after proof, τ_{min}, the time to failure without proof, τ_o, and the time to failure after proof, τ, are shown for various P_a and σ_p/σ_a.

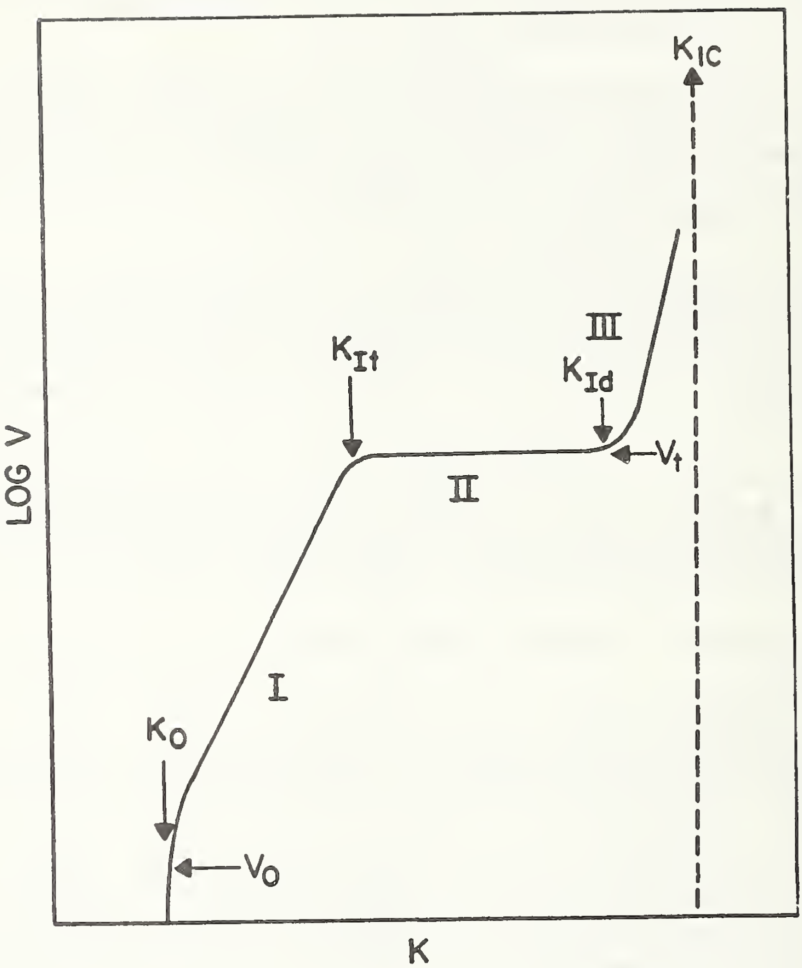

Fig. 1. Schematic representation of the effect of crack tip stress intensity, K_I, on crack velocity, V, during slow crack growth.

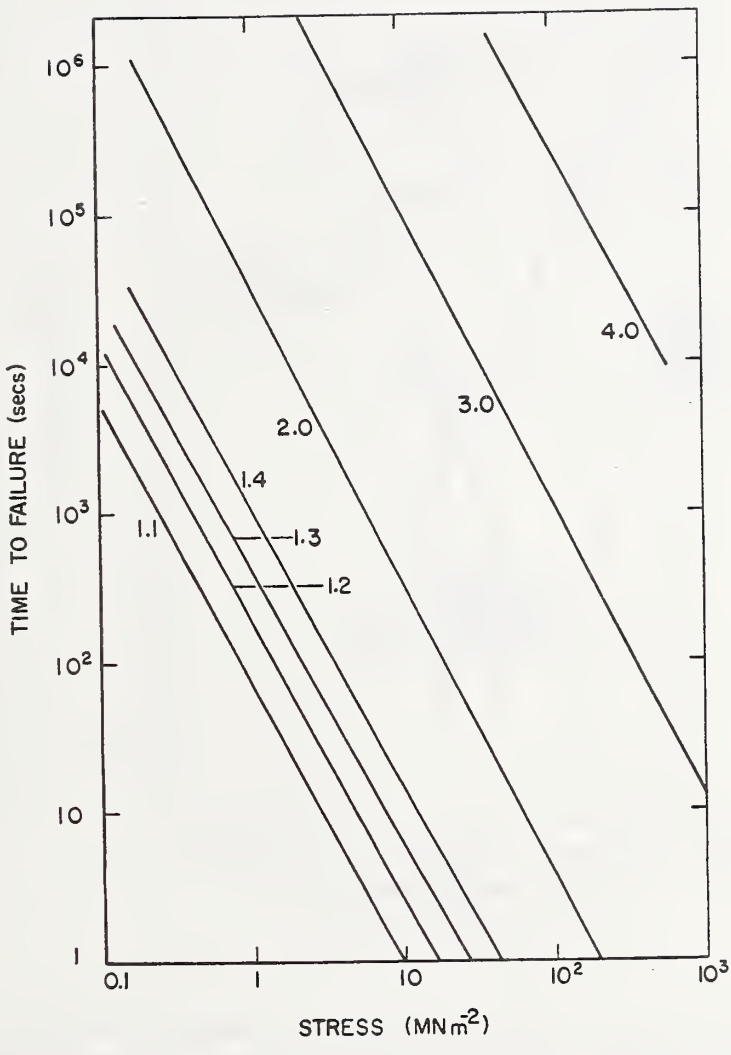

Fig. 2. A proof test diagram for soda-lime glass in water. The numbers below each line refer to the proof stress/applied stress ratio (σ_p/σ_a) corresponding to that line.

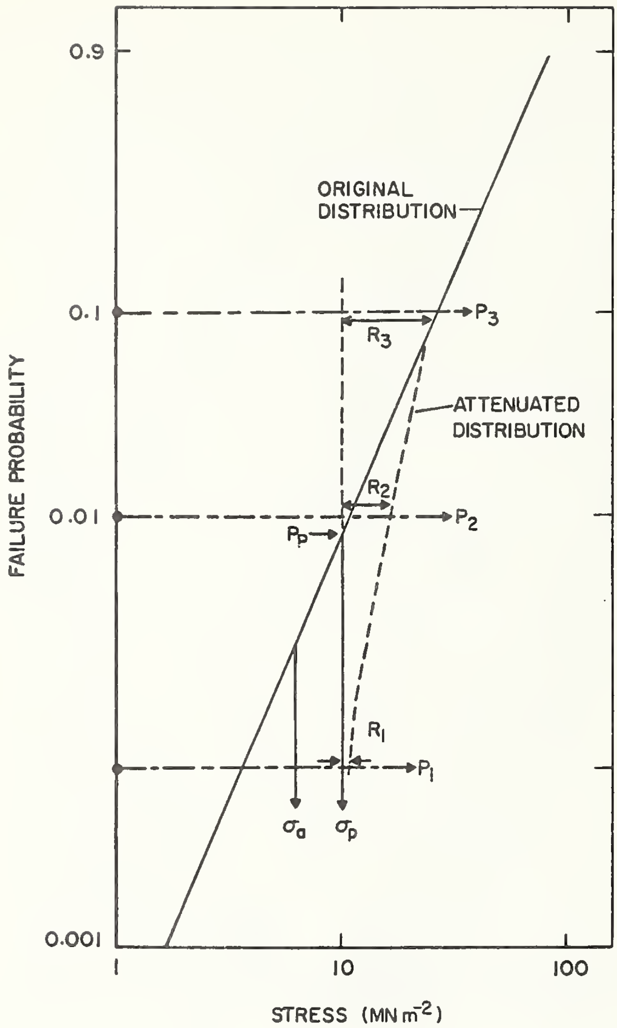

Fig. 3. A typical strength distribution for a ceramic material plotted on Weibull axes. σ_p is the proof stress, σ_a is the applied stress and P_1, P_2, and P_3 are different levels of component failure probability. The quantities R_1, R_2, and R_3 are related to the time-to-failure ratio, τ/τ_{min}.

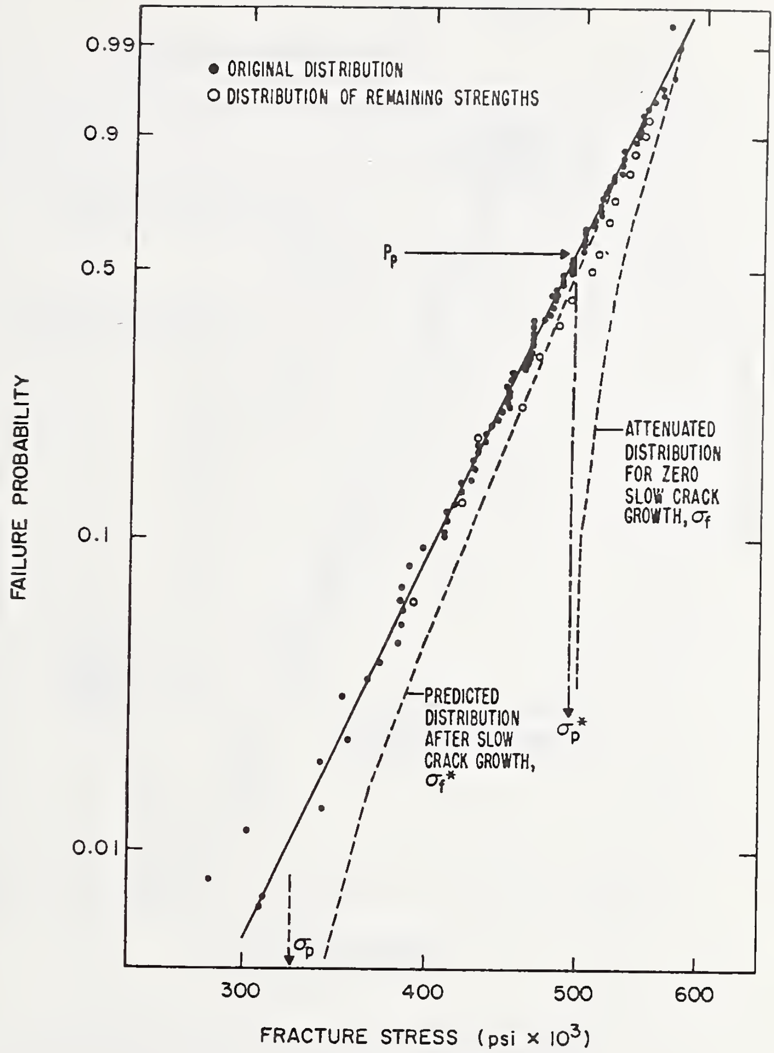

Fig. 4. The strength of E glass fibers before and after a constant stress proof test at σ_p. Also shown are the strengths after proof testing when no slow crack growth occurs, σ_f, and the predicted strengths due to slow crack growth, σ_f^*. Data obtained from reference (17).

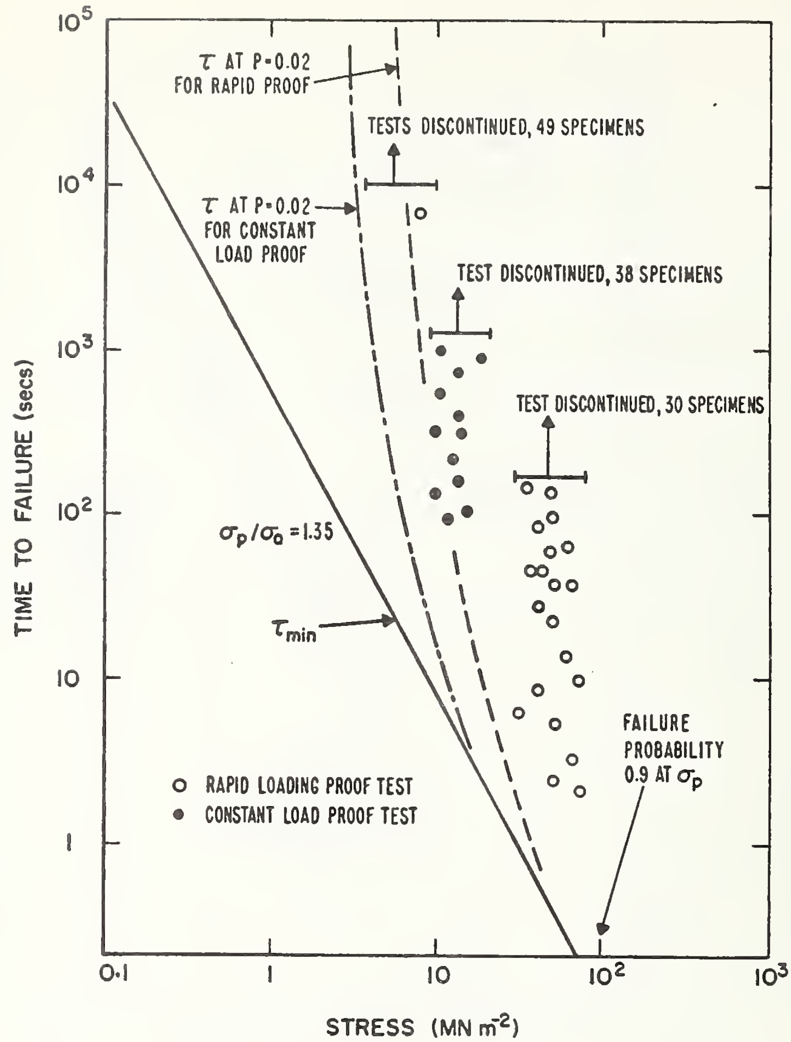

Fig. 5. A comparison of failure times after proof testing for ground soda-lime glass in water, with the predicted minimum failure time for the soda-lime glass/water system (full line), and the times in excess of the minimum for a probability of 0.02.

Fig. 6. The flexural strength distribution of ground soda-lime glass.

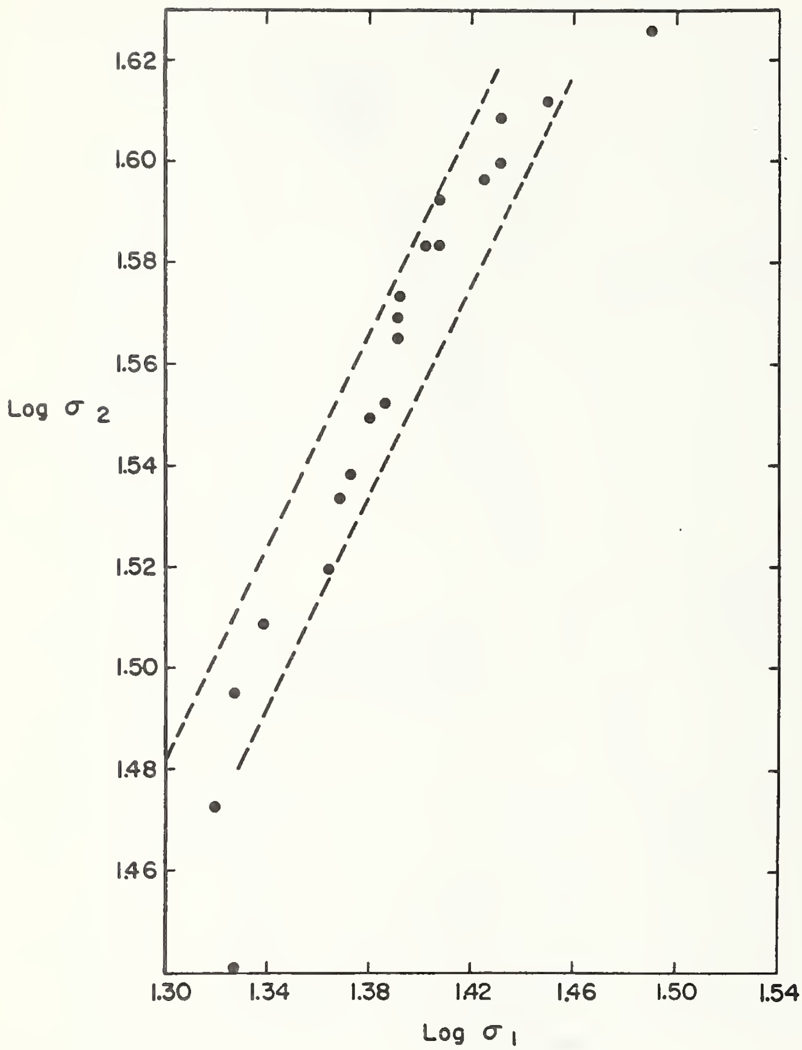

Fig. 7. A logarithmic plot of the strengths, σ, and σ_2 at equivalent probability at two separate strain rates, ε_1 and ε_2 (where $\dot{\varepsilon}_1/\dot{\varepsilon}_2 = 600$). The intercept gives a value for n of 15 ±2.

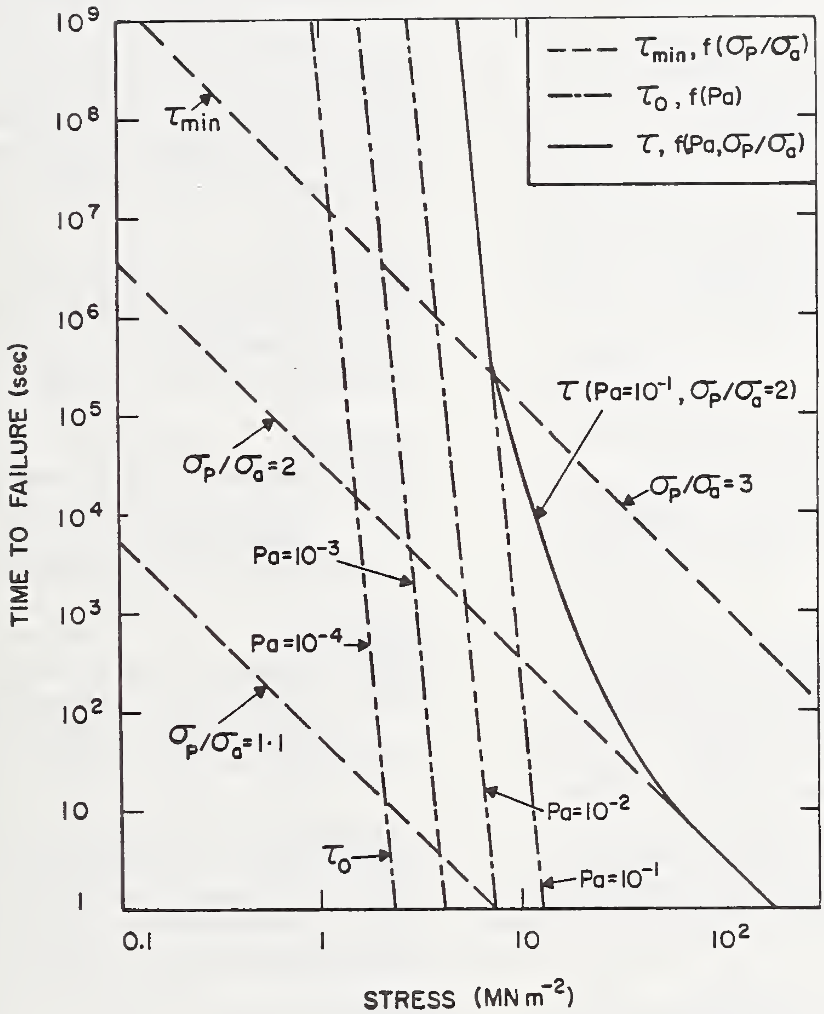

Fig. 8. A complete time-to-failure diagram for ground soda-lime glass immersed in water, under a flexural load. The minimum time to failure after proof, τ_{min}, the time to failure without proof, τ_0, and the time to failure after proof, τ, are shown for various P_a and σ_p/σ_a.

DISTRIBUTION LIST

Organization

Office of Naval Research
Department of the Navy
Attn: Code 471
Arlington, Virginia 22217

Director
Office of Naval Research
Branch Office
495 Summer Street
Boston, Massachusetts 02210

Commanding Officer
Office of Naval Research
New York Area Office
207 West 24th Street
New York, New York 10011

Director
Office of Naval Research
Branch Office
219 South Dearborn Street
Chicago, Illinois 60604

Director
Office of Naval Research
Branch Office
1030 East Green Street
Pasadena, California 91101

Commanding Officer
Office of Naval Research
San Francisco Area Office
50 Fell Street
San Francisco, California 94102

Commanding Officer
Naval Weapons Laboratory
Attn: Research Division
Dahlgren, Virginia 22448

Organization

Director
Naval Research Laboratory
Attn: Technical Information Officer
Code 2000
Washington, D. C. 20390

Director
Naval Research Laboratory
Attn: Technical Information Officer
Code 2020
Washington, D. C. 20390

Director
Naval Research Laboratory
Attn: Technical Information Officer
Code 6000
Washington, D. C. 20390

Director
Naval Research Laboratory
Attn: Technical Information Officer
Code 6100
Washington, D. C. 20390

Director
Naval Research Laboratory
Attn: Technical Information Officer
Code 6300
Washington, D. C. 20390

Director
Naval Research Laboratory
Attn: Technical Information Officer
Code 6400
Washington, D. C. 20390

Director
Naval Research Laboratory
Attn: Library
Code 2029 (ONRL)
Washington, D. C. 20390

Commander
Naval Air Systems Command
Department of the Navy
Attn: Code AIR 320A
Washington, D. C. 20360

Commander
Naval Air Systems Command
Department of the Navy
Attn: Code AIR 5203
Washington, D. C. 20360

Commander
Naval Ordnance Systems Command
Department of the Navy
Attn: Code ORD 033
Washington, D. C. 20360

Commanding Officer
Naval Air Development Center
Aeronautical Materials Div.
Johnsville
Attn: Code MAM
Warminster, Pa. 18974

Commanding Officer
Naval Ordnance Laboratory
Attn: Code 210
White Oak
Silver Spring, Maryland 20910

Commander
Naval Ship Systems Command
Department of the Navy
Attn: Code 0342
Washington, D. C. 20360

Commanding Officer
Naval Civil Engineering Laboratory
Attn: Code L70
Port Hueneme, California 93041

Commander
Naval Ship Engineering Center
Department of the Navy
Attn: Code 6101
Washington, D. C. 20360

Naval Ships R&D Laboratory
Annapolis Division
Attn: Code A800
Annapolis, Maryland 21402

Commanding Officer
Naval Ships R&D Center
Attn: Code 747
Washington, D. C. 20007

U. S. Naval Postgraduate School
Attn: Department of Chemistry
and Material Science
Monterey, California 93940

Commander
Naval Weapons Center
Attn: Code 5560
China Lake, California 93555

Commander
Naval Underseas Warfare Center
Pasadena, California 92152

Scientific Advisor
Commandant of the Marine Corps
Attn: Code AX
Washington, D. C. 20380

Commanding Officer
Army Research Office, Durham
Box CM, Duke Station
Attn: Metallurgy & Ceramics Div.
Durham, North Carolina 27706

Office of Scientific Research
Department of the Air Force
Attn: Solid State Div. (SRPS)
Washington, D. C. 20333

Defense Documentation Center
Cameron Station
Alexandria, Virginia 22314

National Bureau of Standards
Attn: Metallurgy Division
Washington, D. C. 20234

National Bureau of Standards
Attn: Inorganic Materials Div.
Washington, D. C. 20234

Atomic Energy Commission
Attn: Metals & Materials Branch
Washington, D. C. 20545

Argonne National Laboratory
Metallurgy Division
P. O. Box 299
Lemont, Illinois 60439

Brookhaven National Laboratory
Technical Information Division
Attn: Research Library
Upton, Long Island, New York 11973

Library
Bldg. 50, Room 134
Lawrence Radiation Laboratory
Berkeley, California 94720

Los Alamos Scientific Laboratory
P. O. Box 1663
Attn: Report Librarian
Los Alamos, New Mexico 87544

Commanding Officer
Army Materials and Mechanics
Research Center
Attn: Res. Programs Office (AMXMR-P)
Watertown, Massachusetts 02172

Director
Metals & Ceramics Division
Oak Ridge National Laboratory
P. O. Box X
Oak Ridge, Tennessee 37830

Commanding Officer
Naval Underwater Systems Center
Newport, Rhode Island 02844

Aerospace Research Laboratories
Wright-Patterson AFB
Building 450
Dayton, Ohio 45433

Defense Metals Information Center
Battelle Memorial Institute
505 King Avenue
Columbus, Ohio 43201

Army Electronics Command
Evans Signal Laboratory
Solid State Devices Branch
c/o Senior Navy Liaison Officer
Fort Monmouth, New Jersey 07703

Commanding General
Department of the Army
Frankford Arsenal
Attn: ORDBA-1320, 64-4
Philadelphia, Pennsylvania 19137

Executive Director
Materials Advisory Board
National Academy of Sciences
2101 Constitution Avenue, N. W.
Washington, D. C. 20418

NASA Headquarters
Attn: Code RRM
Washington, D. C. 20546

Air Force Materials Lab
Wright-Patterson AFB
Attn: MAMC
Dayton, Ohio 45433

Air Force Materials Lab
Wright-Patterson AFB
Attn: MAAM
Dayton, Ohio 45433

Deep Submergence Systems Project
Attn: DSSP-00111
Washington, D. C. 20360

Advanced Research Projects Agency
Attn: Director, Materials Sciences
Washington, D. C. 20301

Army Research Office
Attn: Dr. T. E. Sullivan
3045 Columbia Pike
Arlington, Virginia 22204

Department of the Interior
Bureau of Mines
Attn: Science & Engineering Advisor
Washington, D. C. 20240

Defense Ceramics Information Center
Battelle Memorial Institute
505 King Avenue
Columbus, Ohio 43201

National Aeronautics & Space Adm.
Lewis Research Center
Attn: Librarian
21000 Brookpark Rd.
Cleveland, Ohio 44135

Naval Missile Center
Materials Consultant
Code 3312-1
Point Mugu, California 93041

Commanding Officer
Naval Weapons Center Corona Labs.
Corona, California 91720

Commander
Naval Air Test Center
Weapons Systems Test Div. (Code 01A)
Patuxent River, Maryland 20670

Director
Ordnance Research Laboratory
P. O. Box 30
State College, Pennsylvania 16801

Director
Applied Physics Laboratory
Johns Hopkins University
8621 Georgia Avenue
Silver Spring, Maryland 20901

Director
Applied Physics Laboratory
1013 Northeast Fortieth St.
Seattle, Washington 98105

Materials Sciences Group
Code S130.1
271 Catalina Boulevard
Navy Electronics Laboratory
San Diego, California 92152

Dr. Waldo K. Lyon
Director, Arctic Submarine Laboratory
Code 90, Building 371
Naval Undersea R&D Center
San Diego, California 92132

Dr. R. Nathan Katz
Ceramics Division
U.S. Army Materials & Mechanics
Research Center
Watertown, Mass. 02172

SUPPLEMENTARY DISTRIBUTION LIST

Professor R. Roy
Materials Research Laboratory
Pennsylvania State University
University Park, Pennsylvania 16802

Professor D. H. Whitmore
Department of Metallurgy
Northwestern University
Evanston, Illinois 60201

Professor J. A. Pask
Department of Mineral Technology
University of California
Berkeley, California 94720

Professor D. Turnbull
Div. of Engineering and Applied Science
Harvard University
Pierce Hall
Cambridge, Massachusetts 02100

Dr. T. Vasilos
AVCO Corporation
Research and Advanced Development Div.
201 Lowell Street
Wilmington, Massachusetts 01887

Dr. H. A. Perry
Naval Ordnance Laboratory
Code 230
Silver Spring, Maryland 20910

Dr. Paul Smith
Crystals Branch, Code 6430
Naval Research Laboratory
Washington, D. C. 20390

Dr. A. R. C. Westwood
RIAS Division
Martin-Marietta Corporation
1450 South Rolling Road
Baltimore, Maryland 21227

Prof. M. H. Manghnani
University of Hawaii
Hawaii Institute of Geophysics
2525 Correa Road
Honolulu, Hawaii 96822

Dr. R. H. Doremus
General Electric Corporation
Metallurgy and Ceramics Lab.
Schenectady, New York 12301

Professor G. R. Miller
Department of Ceramic Engineering
University of Utah
Salt Lake City, Utah 84112

Dr. Philip L. Farnsworth
Materials Department
Battelle Northwest
P. O. Box 999
Richland, Washington 99352

Mr. G. H. Heartling
Ceramic Division
Sandia Corporation
Albuquerque, New Mexico 87101

Mr. I. Berman
Army Materials and Mechanics
Research Center
Watertown, Massachusetts 02171

Dr. F. F. Lange
Westinghouse Electric Corporation
Research Laboratories
Pittsburgh, Pennsylvania 15235

Professor H. A. McKinstry
Pennsylvania State University
Materials Research Laboratory
University Park, Pa. 16802

Professor T. A. Litovitz
Physics Department
Catholic University of America
Washington, D. C. 20017

Dr. R. J. Stokes
Honeywell, Inc.
Corporate Research Center
500 Washington Avenue, South
Hopkins, Minnesota 55343

Dr. W. Haller
Chief, Inorganic Glass Section
National Bureau of Standards
Washington, D.C. 20234

Dr. Harold Liebowitz
Dean of Engineering
George Washington University
Washington, D. C. 20006

Dr. H. Kirchner
Ceramic Finishing Company
P. O. Box 498
State College, Pennsylvania 16801

Professor A. H. Heuer
Case Western Reserve University
University Circle
Cleveland, Ohio 44106

Dr. D. E. Niesz
Battelle Memorial Institute
505 King Avenue
Columbus, Ohio 43201

Dr. F. A. Kroger
University of Southern California
University Park
Los Angeles, California 90007

Dr. Sheldon M. Wiederhorn
National Bureau of Standards
Inorganic Materials Division
Washington, D.C. 20234

Dr. C. O. Hulse
United Aircraft Research Labs
United Aircraft Corporation
East Hartford, Connecticut 06108

Dr. R. M. Haag
Space Systems Division
AVCO Corporation
Lowell Industrial Park
Lowell, Massachusetts 01851

Dr. Stephen Malkin
Department of Mechanical Engineering
University of Texas
Austin, Texas 78712

Prof. H. E. Wilhelm
Department of Mechanical Engineering
Colorado State University
Fort Collins, Colorado 80521

Stanford University
Dept. of Materials Sciences
Stanford, California 94305

Dr. R. K. MacCrone
Department of Materials Engineering
Rensselaer Polytechnic Institute
Troy, New York 12181

Dr. D. C. Mattis
Belfer Graduate School of Science
Yeshiva University
New York, New York 10033

Professor R. B. Williamson
College of Engineering
University of California
Berkeley, California 94720

Professor R. W. Gould
Department of Metallurgical
and Materials Engineering
College of Engineering
University of Florida
Gainesville, Florida 32601

Professor V. S. Stubican
Department of Materials Science
Ceramic Science Section
Pennsylvania State University
University Park, Pennsylvania 16802

Dr. R. C. Anderson
General Electric R and D Center
P. O. Box 8
Schenectady, New York 12301

Dr. Bert Zauderer
MHD Program, Advanced Studies
Room L-9513 - VFSC
General Electric Company
P. O. Box 8555
Philadelphia, Penna. 19101

Prof. C. F. Fisher, Jr.
Department of Mechanical and Aerospace Engineering
University of Tennessee
Knoxville, Tennessee 37916

FORM NBS-114A (1-71)

U.S. DEPT. OF COMM. BIBLIOGRAPHIC DATA SHEET	1. PUBLICATION OR REPORT NO. NBSIR 73-147	2. Gov't Accession No.	3. Recipient's Accession No.
4. TITLE AND SUBTITLE Proof Testing of Ceramic Materials--An Analytical Basis for Failure Prediction			5. Publication Date March 1973 6. Performing Organization Code
7. AUTHOR(S) A. G. Evans and S. M. Wiederhorn			8. Performing Organization NBSIR 73-147
9. PERFORMING ORGANIZATION NAME AND ADDRESS NATIONAL BUREAU OF STANDARDS DEPARTMENT OF COMMERCE WASHINGTON, D.C. 20234			10. Project/Task/Work Unit No. 3130453 11. Contract/Grant No. NR 032-517
12. Sponsoring Organization Name and Address Office of Naval Research Department of the Navy Arlington, Virginia 22217			13. Type of Report & Period Covered Interim 14. Sponsoring Agency Code

15. SUPPLEMENTARY NOTES

16. ABSTRACT (A 200-word or less factual summary of most significant information. If document includes a significant bibliography or literature survey, mention it here.)

An analysis is presented which permits the accurate prediction of component lifetimes after proof testing. The analysis applies to crack propagation controlled fracture but can be used as a conservative prediction when crack initiation is predominant. The analytical predictions are confirmed in a series of time-to-failure measurements.

17. KEY WORDS (Alphabetical order, separated by semicolons)
Ceramics; failure probability; minimum time-to-failure; proof stress diagrams; proof testing.

18. AVAILABILITY STATEMENT	19. SECURITY CLASS (THIS REPORT)	21. NO. OF PAGES
[X] UNLIMITED.	UNCLASSIFIED	
[ ] FOR OFFICIAL DISTRIBUTION. DO NOT RELEASE TO NTIS.	20. SECURITY CLASS (THIS PAGE) UNCLASSIFIED	22. Price